Photochemistry and Photobiology
The official journal of the American Society of Photobiology

Spectroscopy, Microscopy and Fluorescence Imaging of Origanum vulgare L. Basis for Non-destructive Quality Assessment

Journal:	*Photochemistry and Photobiology*
Manuscript ID:	PHP-2013-03-SIPRA-0066.R1
Wiley - Manuscript type:	Symposium-in-Print: Research Article
Date Submitted by the Author:	15-May-2013
Complete List of Authors:	Mendes Novo, Johanna; University of Buenos Aires, Química Inorgánica, Analítica y Química Física Iriel, Analia; University of Buenos Aires, Centro de Estudios Transdisciplinarios del agua Marchi, María; University of Buenos Aires, Química Inorgánica, Analítica y Química Física Lagorio, María; University of Buenos Aires, INQUIMAE/Química Inorgánica, Analítica y Química Física
Keywords:	Fluorescence, SEM, Origanum, ATR-IR

SCHOLARONE™
Manuscripts

Spectroscopy, Microscopy and Fluorescence Imaging of *Origanum vulgare* L. Basis for Non-destructive Quality Assessment.

Johanna Mendes Novo [1], Analia Iriel [2], M. Claudia Marchi [1,3], M. Gabriela Lagorio*[1].

[1]. INQUIMAE / Dpto. de Química Inorgánica, Analítica y Química Física. Facultad de Ciencias Exactas y Naturales. Universidad de Buenos Aires. Ciudad Universitaria. Pabellón II, 1er piso, C1428EHA, Buenos Aires, Argentina, [2]. Centro de Estudios Transdisciplinarios del Agua, Facultad de Ciencias Veterinarias, Universidad de Buenos Aires, Av. Chorroarín 280, C1427CWO, Buenos Aires, Argentina, [3]. Centro de MicroscopíasAvanzadas. Facultad de Ciencias Exactas y Naturales. Universidad de Buenos Aires. Ciudad Universitaria. Pabellón I, 1er piso, C1428EHA, Buenos Aires, Argentina

*Corresponding author e-mail: mgl@qi.fcen.uba.ar (María Gabriela Lagorio)

For Peer Review

ABSTRACT

The organs of *Origanum vulgare* L. plant were examined by optical microscopy, scanning electron microscopy and autofluorescence imaging. The different organs were also studied spectroscopically. Fluorescence emission spectra were recorded for intact inflorescences, leaves and stems. Several fluorescence ratios (Blue/Red, Blue/Far-red, Green/Red and Green/Far-red), which varied depending on the considered organ of the plant, were derived. For leaves, a dependence of fluorescence spectra with water content was obtained as well. The intact samples were also analysed by Attenuated Total Reflectance Fourier Transform Infrared Spectroscopy. These spectra were transformed to the Remission function depending on the wavenumber and two absorption bands (811 cm^{-1} and 1740 cm^{-1}), which displayed differences according to the plant organ sampled, were detected. These results were consistent with higher carvacrol content in inflorescences. The spectroscopic results were connected with the microscopic observation and with the presence of relevant nutraceutics contained in the plant. The optical indexes derived in this work may serve as potential indicators to be explored in the development of non-destructive methods for oregano quality assessment.

INTRODUCTION

For Peer Review

Origanum vulgare L. is an herb belonging to the Labiatae family with relevant properties in the fields of medicine, food flavors, cosmetics and fragrance industry (1). Oregano has been used in traditional medicine to treat diseases of the respiratory apparatus and the urinary tract as well as in menstrual disorders (2-4). Its medicinal properties are usually attributed to the content of different antioxidant compounds. In fact, the essential oil (rich in phenolic monoterpenes as carvacrol) and the aqueous extract, containing polyphenols (mainly rosmarinic acid) and flavonoids, have shown a protective effect against lipoproteins oxidation (5). This plant has also been extensively studied regarding its antimicrobial (6), and antifungal (7) properties. However, there is a vacancy in literature for spectroscopic studies of this species, especially in intact samples.

There is currently much interest in applying non-destructive electromagnetic irradiation on intact biological tissues and get information about the sample from the analysis of the photons given off by the material as a product of this interaction. In the present work we studied spectroscopically different organs of oregano plant with the aim of finding out optical indicators that could differentiate the diverse organs of the plant and that could be related furthermore to the presence of nutraceuticals. Additionally we have analyzed microscopically the sites where these optical signals originated. As oregano is normally purchased as a dry herb (mixture of leaves and inflorescences with a maximum 3% of stems) (8) special focus on the spectroscopy of dry samples was done.

MATERIALS AND METHODS

For Peer Review

Samples: Experiments were performed on dry leaves, inflorescences and stems of oregano plant. Intact leaves with different water content were also studied. Oregano essential oil was obtained from dry leaves and inflorescences by steam distillation. When mentioning dry samples, we refer to samples with around 10% moisture (average commercial degree of humidity).

Drying: Oregano samples were dried in oven at 100-105°C during 24 hs and the moisture content was determined by weight difference. Samples with different moisture content were prepared varying the residence time in the drying oven.

Optical microscopy: Fresh and dry organs of Oregano plant were observed with a Bresser Biolux AL optical microscope (objectives 4X/10X/40X) in both transmission and reflection modes and the images were captured with a SONY Cybershot DSCW150/R 8.1MP Digital Camera.

Scanning electron microscopy: Images were captured on dehydrated samples using a Scanning Electron Microscope (SEM) Zeiss Supra 40 equipped with a field emission gun. The images were taken with in-lens detector and acceleration voltage of 3 kV, at 10^{-6} mbar vacuum chamber. False colors were used for a better observation. The samples were placed on an aluminum holder, supported on conductive carbon tape and coated by sputtering with 15 nm gold layer.

Fluorescence imaging microscopy: Autofluorescence images were captured with an inverted microscope Olympus IX-71 equipped with a X-cite 120 PC fluorescence illumination system and a cooled EMCCD camera Andor iXon3 885 K-VP. A Zeiss plan 10X 0.22 microscope objective was used. For blue fluorescence imaging (blue channel): Excitation 400-450 nm; Omega Filters XF1009 (425DF45), Dichroic Omega Filters 475DCLP; Emission 470-495 nm; Semrock FF02-482/48-15. For the green fluorescence imaging (green channel): Excitation 330-385 nm; BP 330-385, Dichroic DM400 LP, both from set Olympus U-MWU2; Emission 505-535 nm; Semrock

For Peer Review

FF02-520/28-15.

Fluorescence emission spectroscopy: Fluorescence spectra of the different organs of oregano plant were obtained using a steady-state spectrofluorometer (QuantaMaster, PTI -Photon Technology International- Brunswick, USA) in front face geometry. A 75 Watt Xenon lamp was used as the excitation source and the incidence and detection angles were set to 30° and 60° respectively. The excitation wavelength was set to 400 nm, as it led to the maximum intensity in blue-green fluorescence. Emission spectra were recorded from 420 to 780 nm and they were corrected for the detector response to different wavelengths. Fluorescence spectra were recorded for layers of the dry material (inflorescences, leaves and stems). Emission from fresh leaves as a function of their water content was also studied. For comparison purposes, the fluorescence emission spectrum for a dilute ethanolic solution[1] of the oregano essential oil was also obtained exciting at 275 nm, recording emission spectrum from 290 to 500 nm. In this case, a 10 mm-pathlength cuvette was used and the emission was detected at 90° from the excitation beam. Intact oregano samples were also excited in front face at 275 nm and their emissions were recorded from 295 to 500 nm.

Attenuated total reflectance Fourier transform infrared spectroscopy: Mid-IR Spectra were recorded on a Nicolet 8700 Fourier transform infrared (FTIR) (Thermo Scientic) spectrometer equipped with Diamond crystal, deuterated triglyceride sulfate (DTGS) detector spectrometer from 350 to 4000 cm^{-1}. All spectra were collected for 64 scans at a resolution of 4 cm^{-1} in a range of 4000-400 cm^{-1} with a 100 cm aperture. Spectra were referenced to a background spectrum previously recorded on the crystal without plant material. The working temperature was 24ºC. Obtained data were processed with the Software OMNIC versión 7.3

For Peer Review

Thermo Electron Corporation. Either one drop of essential oil (about 10 μL) or some miligrams (2-10 mg) of the solid oregano were placed on the surface of the diamond–ZnSe–ATR crystal used in the determinations. A pressure applicator on the sample allowed an intimate contact between it and the sensing device. Under these conditions the recorded spectra gave information on the surface layer up to 2-5 μm deep. The reflectance data at each wavelength (R_λ) was transformed to the remission function (F(R)) according to equation (1):

$$F(R) = \frac{(1 - R_\lambda{}^2)}{2R_\lambda} \qquad (1)$$

The remission function represents the sample absorption, being proportional to the chromophore concentration in the solid phase (9).

RESULTS AND DISCUSSION

Optical microscopy

To get microscopic information about fresh samples, optical microscopy by reflected and/or transmitted light was used. In Figure 1, a typical reflection image for an oregano fresh leaf is shown. Glandular trichomes are seen as reddish-yellow drops on the green leaf surface while non- glandular trichomes appear as colorless hairs (Figure 1). Non glandular trichomes have been observed in detail by transmission and an interesting difference was found between fresh

[1] Absorbance lower than 0.05 at 275 nm

For Peer Review

(Figure 2a) and dried leaves (Figure 2b). In fact, the aspect of fresh hairs was homogeneous while dried hairs appeared collapsed displaying nodes and higher light scattering.

<Figure 1>

<Figure 2>

Scanning electron microscopy (SEM)

SEM images were obtained for dried samples of inflorescences, flowers, leaves and stems. The images are presented in false colors in Figures 3 to 6. Details on the glandular (Figure 3c) and non glandular trichomes (Figure 6c) are specially emphasised.

<Figure 3>

<Figure 4>

<Figure 5>

<Figure 6>

Peltate glandular trichomes (10) are observed in the aerial organs of oregano plant (Figures 3-6). Their sizes are about 80-90 μm (Figure 3c). Similar sizes were published for glandular trichomes in mints that were reported to be about 100 μm in diameter (11). These glandular trichomes are the place where biosynthesis and storage of essential oils, rich in monoterpenoid phenols as carvacrol, occur (12, 13). The essential oil content is one of the parameters to evaluate the oregano quality and so the density in glandular trichomes may be related to its grade. In fact, it has been reported that the number of glandular trichomes is

For Peer Review

linearly correlated to the amount of essential oil delivered from the plant (14). From the SEM images, it can be seen that glandular-trichomes density is higher for the inflorescence (floral bracts and flowers), followed by leaves and stems. The distribution of glandular trichomes in leaves is more homogeneous than in stems where the trichomes density is somewhat variable.

Non glandular multicellular trichomes are also present displaying lengths about 200-300 μm (Figure 6c). These trichomes present ridges and internodes in the dried samples and their appearance is similar to that reported for *Salvia chrysophylla* (15).

Fluorescence imaging microscopy

Observation of the dry samples under excitation around 400 nm, showed blue and green emission from the plant tissue except from glandular trichomes that looked dark under these conditions (Figure 7). For fresh leaves, blue-green emission was strongly reduced and the corresponding fluorescence image was weak (image not shown).

<Figure 7>

Fluorescence spectroscopy

Fluorescence spectra from the different organs of oregano excited at 400 nm have essentially shown two types of emission: one in the blue-green region (about 480 nm and 530 nm) and the other in the red-far red portion of spectra (680 and 735 nm) (Figure 8).

<Figure 8>

Chlorophyll-a is responsible for the observed red (680 nm) and far-red (735 nm) emission (16-19). On the other hand, many components, with beneficial health properties and which are reported to be present in oregano, are known to emit blue or green fluorescence:

For Peer Review

phenolic acids as rosmarinic (20), ferulic, p-coumaric (21), chlorogenic and caffeic acids (22), and flavonoids as quercetin (23) and kaempferol (1).

As reported in literature, rosmarinic acid in methanol-water mixture at pH 7 presents an emission maximum at 440-450 nm (24), ferulic acid emits in the region from 400 to 480 nm depending on the solvent media (25), p-coumaric acid fluoresces from 415 to 445 nm (26), chlorogenic acids in methanol emits around 440 nm (27) and caffeic acid emits at 432 nm (28). Regarding flavonoids, quercetin in cellular milieu was reported to emit fluorescence in the region 500-540 nm (29) and Kaempferol around 520 nm (30). Based on the foregoing, it is expected then that the blue-green fluorescence is connected with the presence of phenolic acids and flavonoids in oregano plant.

Fluorescence ratios of intensities at maxima for shorter to longer wavelengths (Blue/Red, Blue/Far-red, Green/Red and Green/Far-red) are shown in Figure 9 for the different organs of the plant. Bars heights represent average values obtained for seven samples of each organ and the error bars indicate the standard deviation.

<Figure 9>

It may be observed that fluorescence ratios Blue/Red, Blue/Far-red, Green/Red and Green/Far-red were higher for dry leaves than for fresh leaves (Figure 9). Varying water concentration in a controlled manner, it could be seen that Green/ Far-red and Blue/ Far-red ratios strongly depended on the water content of leaves showing a linear relation (Figures 10 and 11 respectively).

<Figure 10>

For Peer Review

<Figure 11>

Additionally, the calculated fluorescence ratios for dry samples were different for the different organs of oregano (Figure 9). So, from Figures 9 to 11, it arises that the fluorescence ratio for shorter to longer wavelengths depended, on one hand, upon the humidity degree of the sample, and on the other hand, at constant humidity it varied according to the considered organ of the plant. The fluorescence ratios for dry stems were similar (Blue/ Red) to that for dry inflorescences or intermediate (Blue/Far-red, Green/Red and Green/Far-red) between those for dry inflorescences and dry leaves. Significative differences (Student test at a level of significance p= 0.05) were found for the different fluorescence ratios among the diverse organs with exception of the ratios Blue/Red and Green/ Red between dry inflorescences and dry stems and for Green/Far-red between dry leaves and dry stems. The Blue/Far-red ratio was the indicator displaying significant differences among all the studied samples. However, the Green/Far-red ratio was the indicator displaying higher variation when comparing dry inflorescences with dry leaves (the two major fractions in commercial oregano). Ratios Blue/Green and Red/Far-red did not present differences among the diverse organs of the plant. (results not shown).

A similar increase in the fluorescence ratio Blue-Green/Red in leaves upon drying has been previously reported in literature for some cryptogamic plant species (31). In these plants, the change was attributed to variations in the optical properties of the material during drying and not to the formation of new fluorescing products because this behavior was reversed (i.e. the fluorescence ratio Blue-Green/Red decreased) during rehydration.

Absolute intensities for the blue fluorescence excited at 400 nm showed the following decreasing order: dry inflorescences (8.1×10^5 a.u.) > dry leaves (7.5×10^5 a.u.) > dry stems

For Peer Review

(3.5×10^5 a.u.) > fresh leaves (2.4×10^5 a.u.). Similar results were obtained for the green emission: dry inflorescences (7.8×10^5 a.u.) > dry leaves (6.5×10^5 a.u.) > dry stems (2.8×10^5 a.u.) > fresh leaves (2.5×10^5 a.u.).

The decrease in red and far-red fluorescence observed for the dry samples compared to fresh leaves (Figure 8) can probably be due to destruction of chlorophyll during drying at 100-105 °C.

To analyse if the fluorescence from intact samples could also be connected with the essential oil content, we obtained the fluorescence spectrum for the distilled oil in ethanol solution. In this case, we found an excitation maximum around 275 nm and an emission maximum in the UV at 323 nm (Figure 12). We explored then the non-destructive detection of the essential oil emission around 320 nm in intact oregano excited at 275nm. Under these conditions we have found UV fluorescence with maxima around 310 nm. The band intensities followed the order: inflorescences (7.6×10^5 a.u.) > dry leaves (4.1×10^5 a.u.) > dry stems (1.8×10^5 a.u.) > fresh leaves (7.5×10^4).These last results are consistent with a higher density of glandular trichomes in inflorescences. Moreover, this analysis showed that the UV fluorescence, which specifically emerged from the essential oil in intact samples, could also serve as a tool for non-destructive monitoring.

<Figure 12>

Attenuated total reflectance Fourier transform infrared spectroscopy

ATR-FTIR spectra for the oregano essential oil is shown in Figure 13 together with the spectra for intact dry leaves and inflorescences.

For Peer Review

<Figure 13>

The band placed at 811 cm^{-1} in the essential oil spectrum corresponds to out of plane C-H wagging vibrations and it is characteristic of carvacrol component (32). This band was also observed in the spectrum of dry inflorescences. On the other hand, the absorption band at 1740 cm^{-1} (absent in the essential oil spectrum but present in inflorescences, is due to acidic C=O and it was attributed in bibliography to the presence of rosmarinic acid (33). We paid special attention to both these absorption bands at 811 cm^{-1} and at 1740 cm^{-1} in the intact samples of oregano. In Figure 14 we show F(R) values for these wavenumbers.

<Figure 14>

Both the 811 cm^{-1} and the 1740 cm^{-1} absorption bands were higher for dry inflorescences than for dry leaves. The result is consistent with a higher content of essential oil in inflorescences compared to leaves as it will be seen from the density of glandular trichomes (which biosynthesize the essential oil) captured by SEM analysis. So, our results indicates that the ATR band at 811 cm^{-1} may be a potential indicator of the essential oil content while the ATR band at 1740 cm^{-1} may be potentially connected with the presence of rosmarinic acid and to the content of hydroxycinnamic acids (28) in general. No relevant information could be extracted from ATR spectra of stems.

CONCLUSIONS

Both glandular and non-glandular trichomes have been found in all the studied organs of the plant. The blue-green fluorescence originated in the epidermis and in non–glandular hairs and it strongly increased upon drying. For leaves, Blue/ Far-red and Green/ Far-red fluorescence

For Peer Review

ratios could be linearly connected to the water content. At constant sample humidity, fluorescence ratios became useful tools to distinguish the different organs of the plant, especially for discriminating between leaves and inflorescences (the two major fractions in the commercial product). Glandular trichomes, containing the essential oil, emitted fluorescence in the UV region (around 310 nm). Additionally, inflorescences have shown higher density of glandular trichomes than other organs of the plant, as it could be clearly seen from SEM images and consequently higher essential oil content. This result agreed with their larger emission at 310 nm in the fluorescence spectra and the higher absorption at 811cm^{-1} at the FTIR-ATR spectra. As a consequence, the FTIR-ATR absorption bands and the fluorescent emission could be explored as non-destructive techniques to assess nutraceutical content.

The spectroscopic information and the optical indicators derived in this manuscript could be used in future works for the development of rapid and non-destructive methods of oregano quality assessment.

ACKNOWLEDGMENTS: The authors are grateful to the University of Buenos Aires (Projects UBACyT X114 and UBACyT 20020100100814) and to the Agencia Nacional de Promoción Científica y Tecnológica (BID 1201/OC-AR PICT 938) for the financial support. JMN is supported by a fellowship from the University of Buenos Aires. AI is Assistant research scientist from The Consejo Nacional de Investigaciones Científicas y Técnicas CONICET. The authors greatly appreciate the valuable assistance of Dr. Guillermo Menéndez from Nanotools and Biosensors Lab -CIHEDECAR-CONICET in the fluorescence imaging experiments. The authors also thank an anonymous reviewer for several suggestions that improved this work.

For Peer Review

REFERENCES

1. Kaurinovic, B., M. Popovic, S. Vlaisavljevic and S. Trivic (2011) Antioxidant Capacity of *Ocimum basilicum* L. and *Origanum vulgare* L. Extracts. *Molecules,* **16**, 7401-7414.

2. Bruneton, J. (1999) *Pharmacognosy, Phytochemistry. Medicinal Plants*. 2nd ed. London-New York.

3. Wang, H., G. J. Provan and K. Helliwell (2004) Determination of rosmarinic acid and caffeic acid in aromatic herbs by HPLC. *Food Chem*., **87**, 307-311.

4. *PDR for Herbal Medicines* (2000) (Edited by J. Gruenwald, T. Brendler and C. Jaenicke), pp. 559-560. Thomson Healthcare Inc., Montvale, NJ.

5. Kulisić, T., A. Krisko, V. Dragović-Uzelac, M. Milos and G. Pifat (2007) The effects of essential oils and aqueous tea infusions of oregano (*Origanum vulgare* L. spp. hirtum), thyme (*Thymus vulgaris* L.) and wild thyme (*Thymus serpyllum* L.) on the copper-induced oxidation of human low-density lipoproteins. *Int. J. Food Sci. Nutr*., **58**, 87-93.

6. Aligiannis, N., E. Kalpoutzakis, S. Mitaku and I. B. Chinou (2001) Composition and antimicrobial activity of the essential oils of two Origanum species. *J. Agric. Food Chem.*, **49**, 4168-4170.

7. Salgueiro, L. R., L. R. C. Cavaleiro, E. Pinto, C. Pina-Vaz, A. G. Rodrigues, A. Palmeira, C. Tavares, S. Costa-de-Oliveira, M. J. Goncalves and J. Martinez de Oliveira (2003**)** Chemical Composition and Antifungal Activity of the Essential Oil of *Origanum virens* on *Candida* Species. *Planta Med*., **69**, 871-874.

8. Código Alimentario Argentino, Chapter XVI, Condimentos vegetales, Art.1226.

For Peer Review

285 9. Wendlandt, W. and H. G. Hecht (1966) Reflectance Spectroscopy. Interscience, New York.

286 10. Osman, A. K. (2012) Trichome micromorphology of egyptian ballota (lamiaceae) with
287 emphasis on its systematic implication. *Pak. J. Bot*., **44**, 33-46.

288 11. Wittstock, U. and J. Gershenzon (2002) Constitutive plant toxins and their role in defense
289 against herbivores and pathogens. *Curr. Opin. Plant Biol.*, **5**, 300-307.

290 12. Gersbach, P. V., S. G. Wyllie and V. Sarafis (2001) A New Histochemical Method for
291 Localization of the Site of Monoterpene Phenol Accumulation in Plant Secretory Structures.
292 *Ann. Bot.*, **88**, 521-525.

293 13. Bosabalidis, A., C. Gabrieli, and I. Niopas (1998) Flavone aglycones in glandular hairs of
294 Origanum X intercedens. *Phytochemistry*, **49**, 1549-1553.

295 14. Kofidis G., A. M. Bosabalidis and M. Moustakas (2003) Contemporary seasonal and
296 altitudinal variations of leaf structural features in Oregano (*Origanum vulgare* L.). *Ann. Bot*.,
297 **92**, 635-645.

298 15. Kahraman, A., F. Celep and M. Dogan (2010) Anatomy, trichome morphology and
299 palynology of *Salvia chrysophylla* Stapf (Lamiaceae). *S. Afr. J. Bot.*, **76**, 187–195.

300 16. Lagorio, M. G. (2011) Chlorophyll fluorescence emission spectra in photosynthetic
301 organisms. In Chlorophyll: Structure, Production and Medicinal Uses, Nova Science
302 Publishers, New York, USA.

303 17. Baker, N. R. (2008) Chlorophyll Fluorescence: A Probe of Photosynthesis In Vivo. *Annual*
304 *Review of Plant Biology*, **59**, 89-113.

For Peer Review

18. Papageorgiou, G. and Govindjee (2004) Chlorophyll a fluorescence-a signature of photosynthesis, Springer, Dordrecht..

19. Maxwell,K. and Johnson, G. N. Chlorophyll fluorescence - a practical guide (2000), *J. Exp. Bot*., **51**, 659-668..

20. McCue, P. and K. Shetty (2004) Inhibitory effects of rosmarinic acid extracts on porcine pancreatic amylase *in vitro*. *Asia Pacific J. Clin. Nutr*., **13**, 101-106.

21. Benavides, V., G. D'Arrigo and J. Pino (2010) Effects of aqueous extract of *Origanum vulgare* L. (Lamiaceae) on the preimplantational mouse embryos. *Rev. peru. biol.,* **17**, 381-384.

22. Wojdyło, A., J. Oszmian´ski and R. Czemerys (2007) Antioxidant activity and phenolic compounds in 32 selected herbs. *Food Chem*., **105**, 940–949.

23. Koukoulitsa, C., A. Karioti, M. C. Bergonzi, G. Pescitelli, L. Di Bari and H. Skaltsa (2006) Polar Constituents from the Aerial Parts of *Origanum vulgare* L. Ssp. *hirtum* Growing Wild in Greece. *J. Agric. Food Chem.*, **54**, 5388–5392.

24. Celik, S. E., M. Özyürek, A. N. Tufan, K. Güçlü and R. Apak (2011) Spectroscopic study and antioxidant properties of the inclusion complexes of rosmarinic acid with natural and derivative cyclodextrins. *Spectrochim. Acta A Mol Biomol. Spectrosc.,* **78**, 1615–1624.

25. Meyer, S., A. Cartelat, I. Moya and Z. G. Cerovic, UV-induced blue-green and far-red fluorescence along wheat leaves: a potential signature of leaf ageing. *J. Exp. Bot.*, **54**, 757-769.

For Peer Review

324 26. Goulas, Y., I. Moya and G. Schmuck (1990) Time-resolved spectroscopy of the blue
325 fluorescence of spinach leaves. *Photosynth. Res*, **25**, 299-307.

326 27. Morales, F., A. Cartelat, A. Alvarez-Fernández, I. Moya and Z. G. Cerovic (2005) Time-
327 Resolved Spectral Studies of Blue-Green Fluorescence of Artichoke (Cynara cardunculus L.
328 Var. Scolymus) Leaves:Identification of Chlorogenic Acid as One of the Major Fluorophores
329 and Age-Mediated Changes. *J. Agric. Food Chem.*, **53**, 9668-9678.

330 28. Trnková, L., I. Boušová, V. Kubíček and J. Dršata (2010) Binding of naturally occurring
331 hydroxycinnamic acids to bovine serum albumin. *Nat. Sci.*, **2**, 563-570.

332 29. Nifli A. P., P. A. Theodoropoulos, S. Munier, C. Castagnino, E. Roussakis, H. E.
333 Katerinopoulos, J. Vercauteren and E. Castanas (2007) Quercetin Exhibits a Specific
334 Fluorescence in Cellular Milieu: A Valuable Tool for the Study of Its Intracellular Distribution,
335 *J Agric Food Chem.,* **55**, 2873-2878.

336 30. Peer, W. A., D. E. Brown, B. W. Tague, G. K. Muday, L. Taiz and A. S. Murphy (2001)
337 Flavonoid Accumulation Patterns of Transparent Testa Mutants of Arabidopsis. *Plant Physiol.*,
338 **126**, 536–554.

339 31. Talcics Z., H. K. Lichtenthaler and Z. Tubal (2000) Fluorescence Emission Spectra of
340 Desiccation-tolerant Cryptogamic Plants During a Rehydration - desiccation Cycle. *J. Plant*
341 *Physiol.*, **156**, 375-379.

342 32. Schulz, H., G. Özkan, M. Baranska, H. Krüger and M. Özcan (2005) Characterisation of
343 essential oil plants from Turkey by IR and Raman spectroscopy. *Vib. Spectrosc.*, **39**, 249–256.

For Peer Review

344 33. Mehrabania, M., M. Shams-Ardakanib, A. Ghannadic, N. G. Dehkordic and S. E. Sajjadi
345 Jazic (2005) Production of Rosmarinic Acid in Echium amoenum Fisch. and C.A. Mey. Cell
346 Cultures. *Iran. J. Pharm. Res.*, **2**, 111-115.

347 FIGURE CAPTIONS

348 **Figure 1.** Oregano fresh leaf observed by optical reflection microscopy.

349 **Figure 2.** Oregano non-glandular trichomes observed by optical transmission microscopy, a)
350 fresh leaf, b) dried leaf.

351 **Figure 3.** SEM image in false colors for the dry floral bracts of oregano. a) 100×, b) 500×, c)
352 2.00K×, detail of a peltate glandular trichome seat on a flat epidermis.

353 **Figure 4.** SEM image in false colors for oregano dry-flowers. a) 100×, b) 500×.

354 **Figure 5.** SEM image in false colors for oregano dry-leaves. a) 100×, b) 500×, c) 2.00K×,
355 detail of peltate glandular trichome seat on a local depression.

356 **Figure 6.** SEM image in false colors for oregano dry-stem. a) 100×, b) 500×, c) 1.00K×, detail
357 of non-glandular trichomes.

358 **Figure 7.** Blue-excited blue and UV-excited green fluorescence images captured for dried
359 inflorescences, dry leaves and dry stems of oregano.

For Peer Review

Figure 8. Fluorescence spectra corrected for the detector response for the different organs of oregano. Excitation wavelength: 400 nm. Dry inflorescences (thick grey line), dry stems (thick black line), dry leaves (fine black line), fresh leaves (dashed line).

Figure 9. Fluorescence ratios for the different organs of oregano. The error bars represent the standard deviation.

Figure 10. Green/ Far-red ratio as a function of water content (mass percentage) in oregano leaves.

Figure 11. Blue/ Far-red ratio as a function of water content (mass percentage) in oregano leaves.

Figure 12. Fluorescence spectra corrected for the detector response for the essential oil of oregano in ethanol solution. Excitation wavelength: 275 nm.

Figure 13. ATR-FTIR spectra for a) the essential oil of oregano distilled from leaves and inflorescences, b) dry leaves, c) dry inflorescences.

Figure 14. Absorption bands at 811 cm^{-1} and 1740 cm^{-1} from ATR-FTIR of dry inflorescences and dry leaves of oregano. The error bars represent the standard deviation

For Peer Review

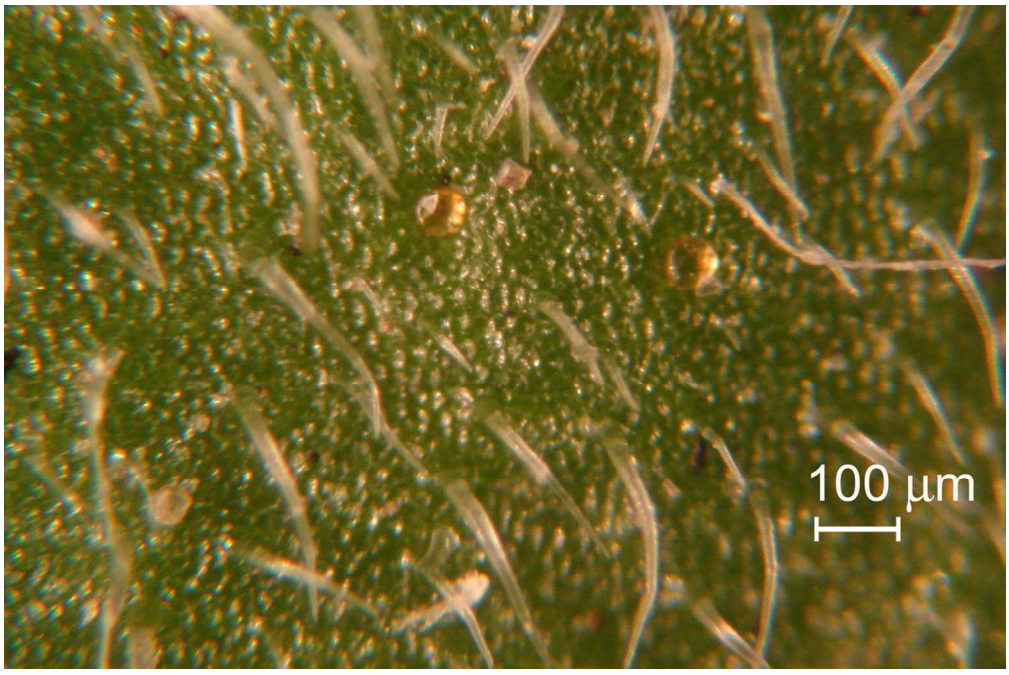

Figure 1. Oregano fresh leaf observed by optical reflection microscopy.
54x36mm (600 x 600 DPI)

Review

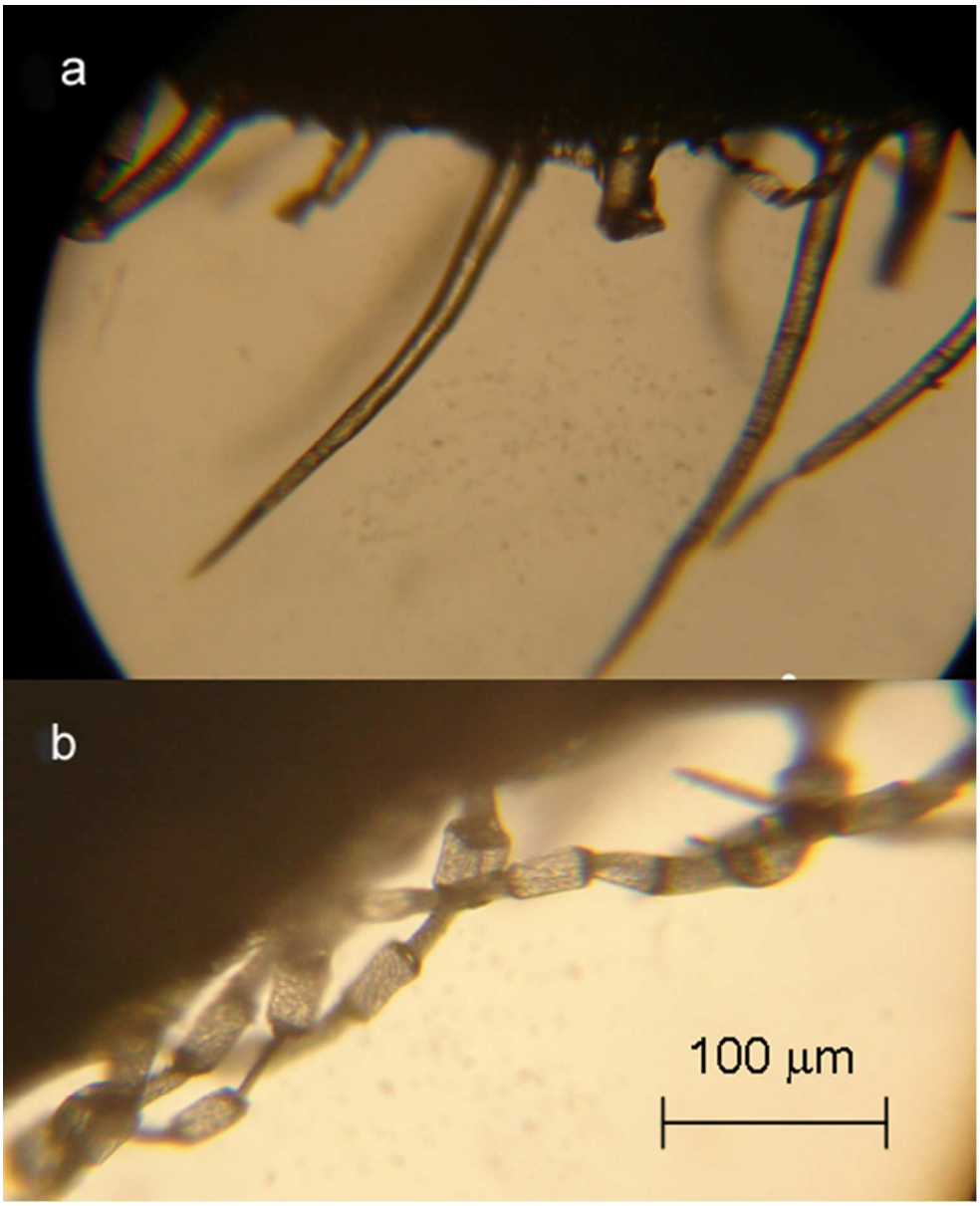

Figure 2. Oregano non-glandular trichomes observed by optical transmission microscopy, a) fresh leaf, b) dried leaf.
82x101mm (150 x 150 DPI)

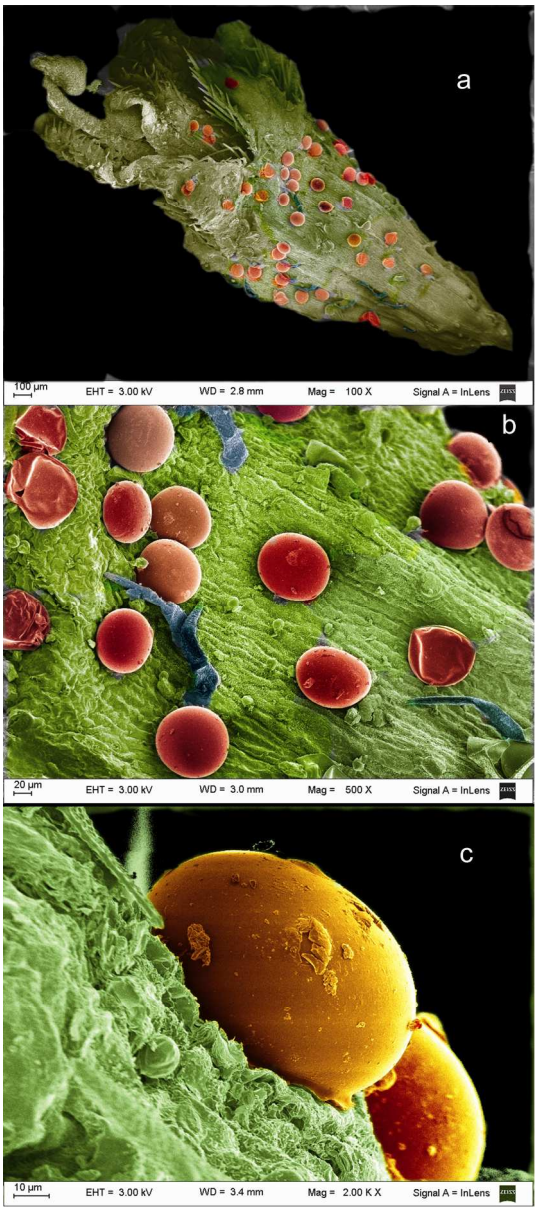

Figure 3. SEM image in false colors for the dry floral bracts of oregano. a) 100×, b) 500×, c) 2.00K×, detail of a peltate glandular trichome seat on a flat epidermis.
187x422mm (300 x 300 DPI)

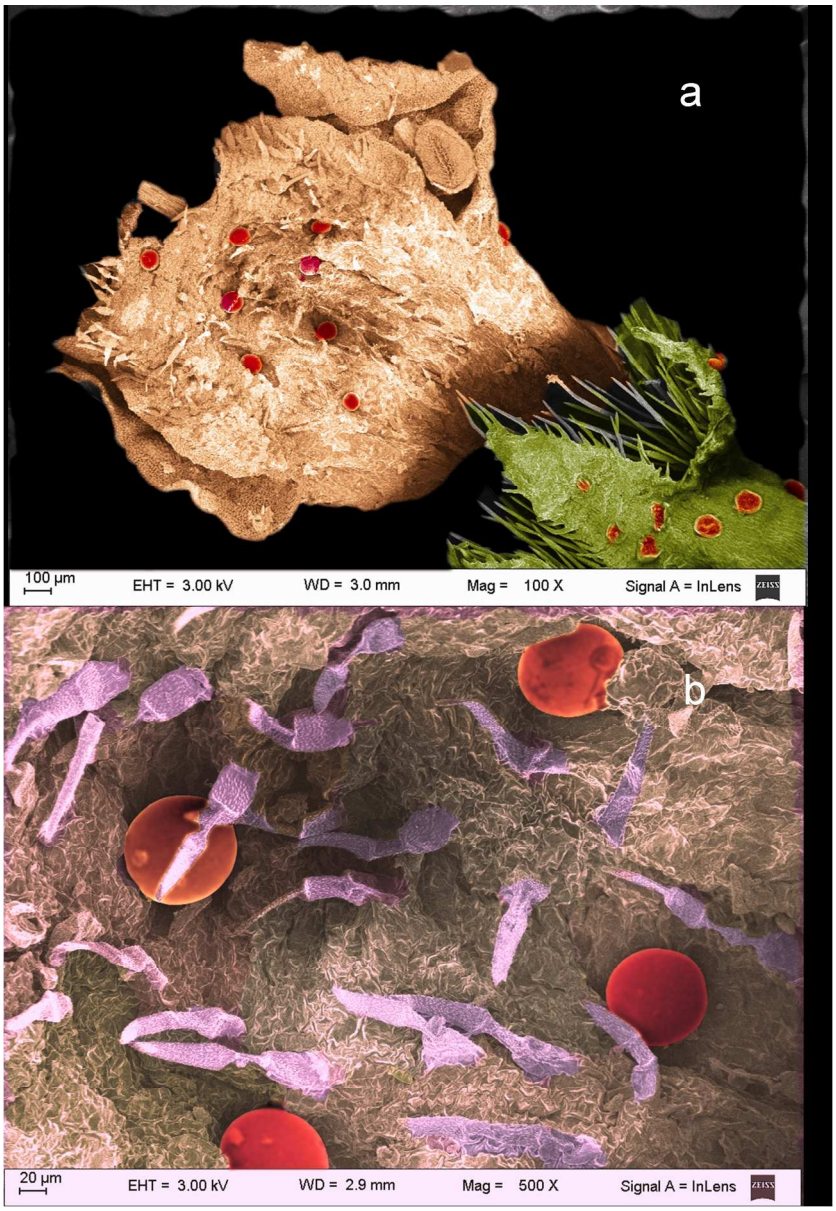

Figure 4. SEM image in false colors for oregano dry-flowers. a) 100×, b) 500×.
120x173mm (600 x 600 DPI)

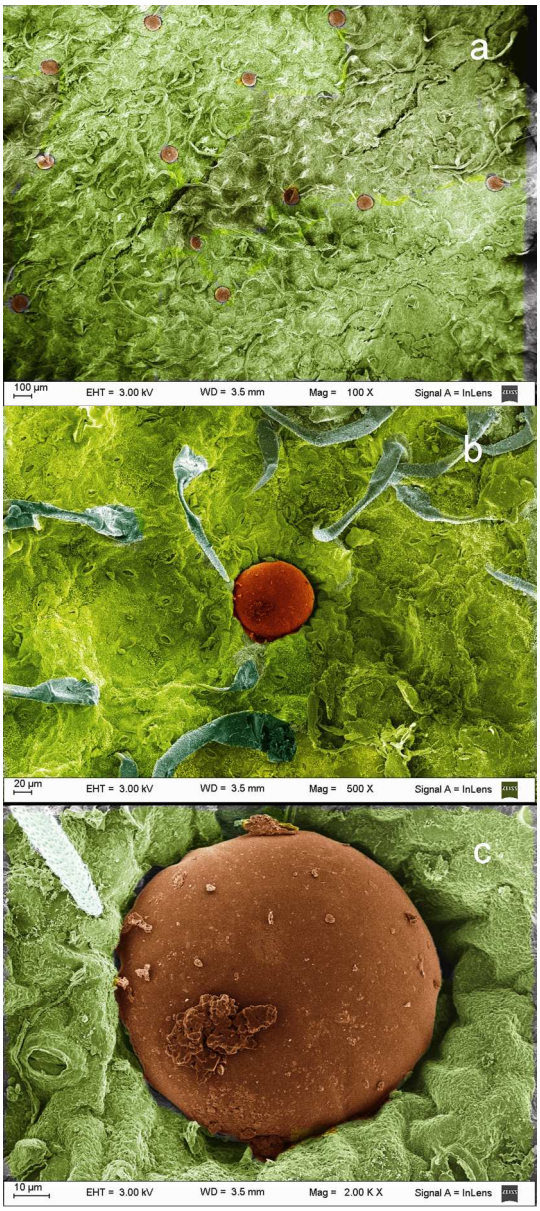

Figure 5. SEM image in false colors for oregano dry-leaves. a) 100×, b) 500×, c) 2.00K×, detail of peltate glandular trichome seat on a local depression.
187x421mm (300 x 300 DPI)

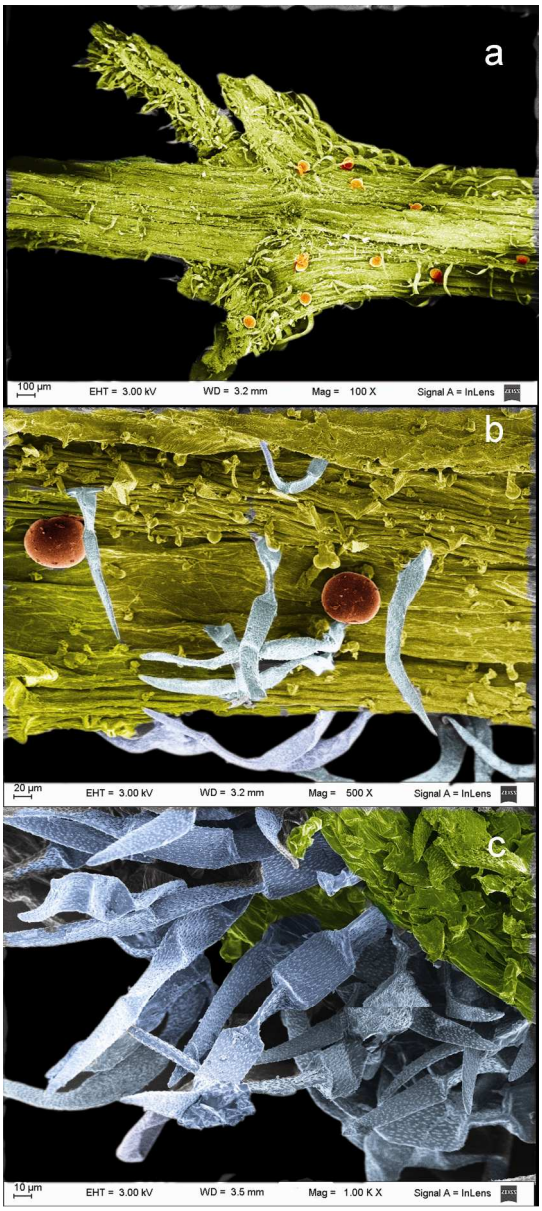

Figure 6. SEM image in false colors for oregano dry-stem. a) 100×, b) 500×, c) 1.00K×, detail of non-glandular trichomes.
186x418mm (300 x 300 DPI)

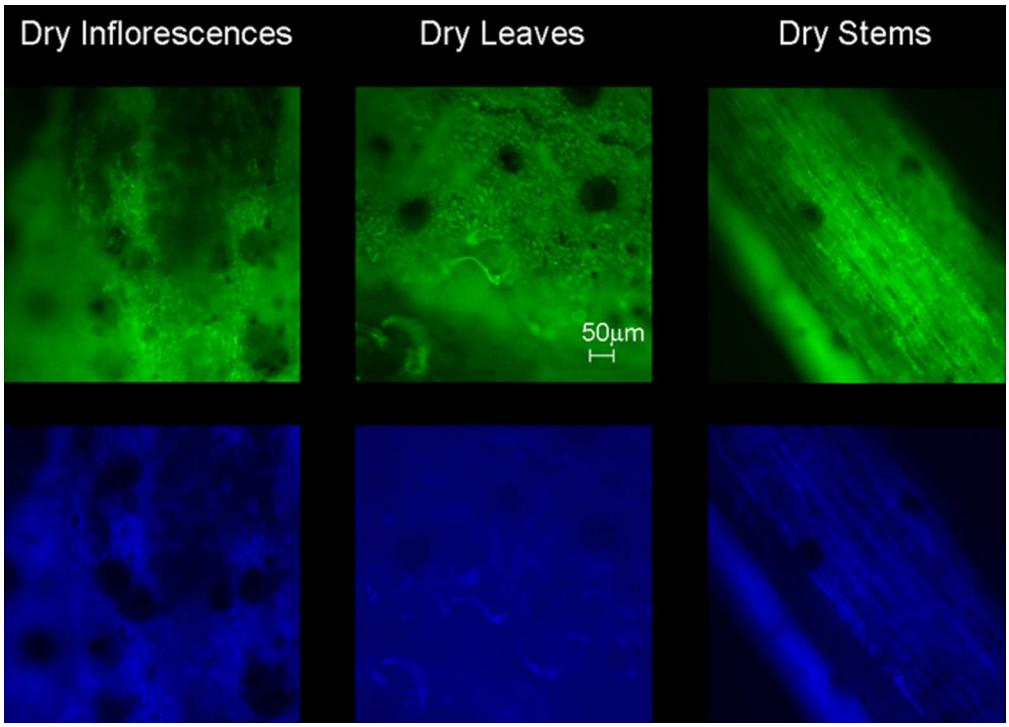

Figure 7. Blue-excited blue and UV-excited green fluorescence images captured for dried inflorescences, dry leaves and dry stems of oregano.
59x42mm (300 x 300 DPI)

Review

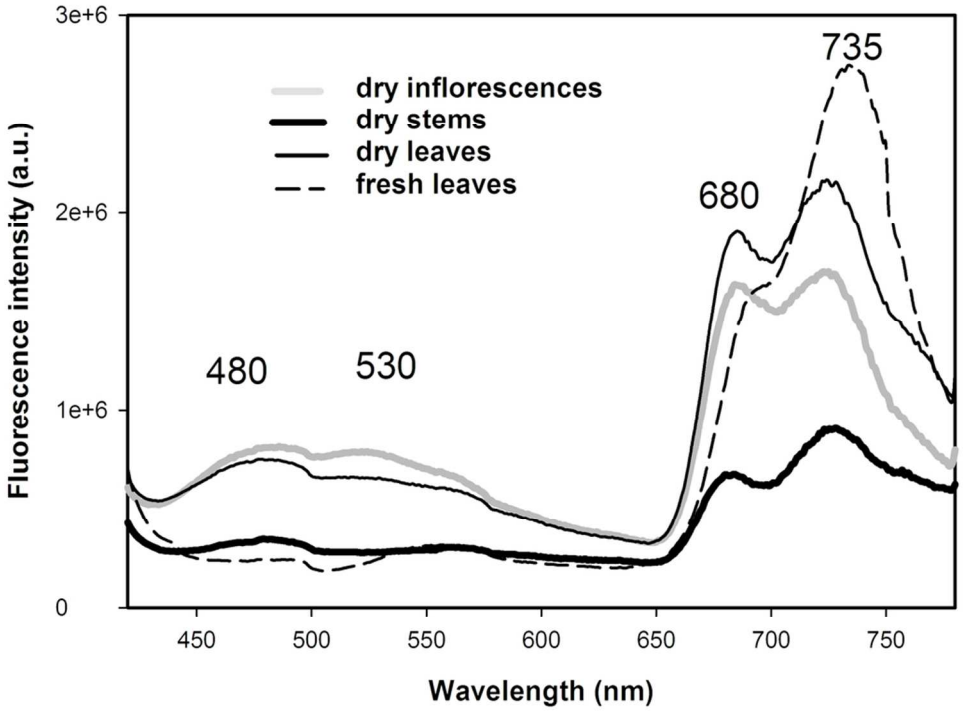

Figure 8. Fluorescence spectra corrected for the detector response for the different organs of oregano. Excitation wavelength: 400 nm. Dry inflorescences (thick grey line), dry stems (thick black line), dry leaves (fine black line), fresh leaves (dashed line).
90x71mm (300 x 300 DPI)

view

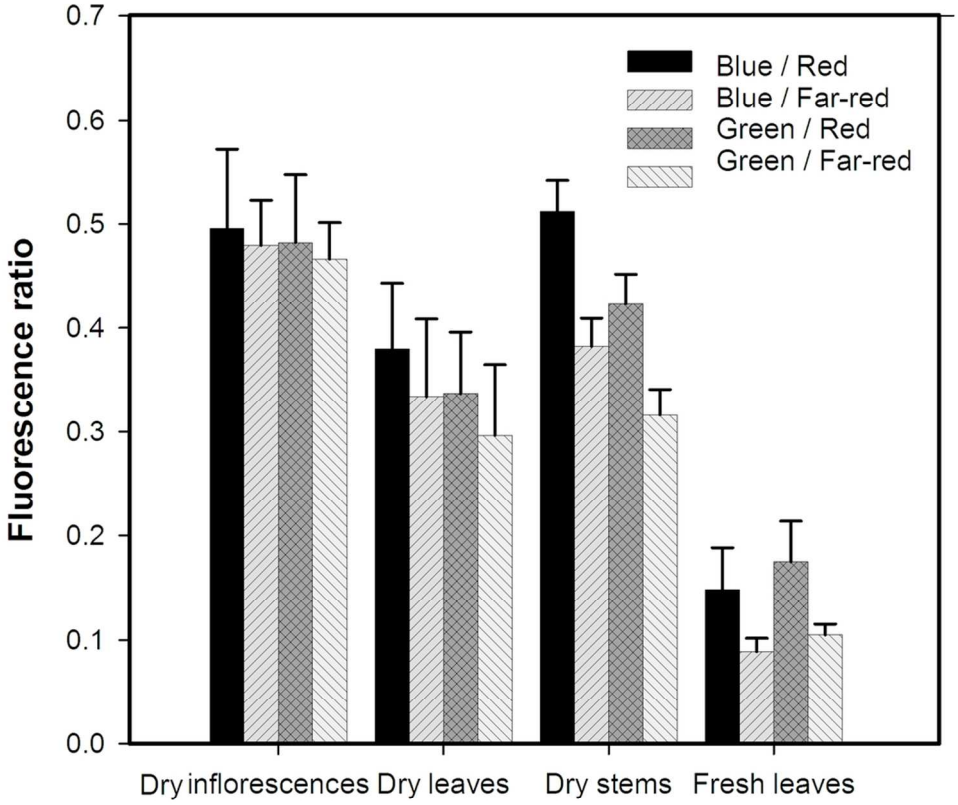

Figure 9. Fluorescence ratios for the different organs of oregano. The error bars represent the standard deviation.
98x116mm (300 x 300 DPI)

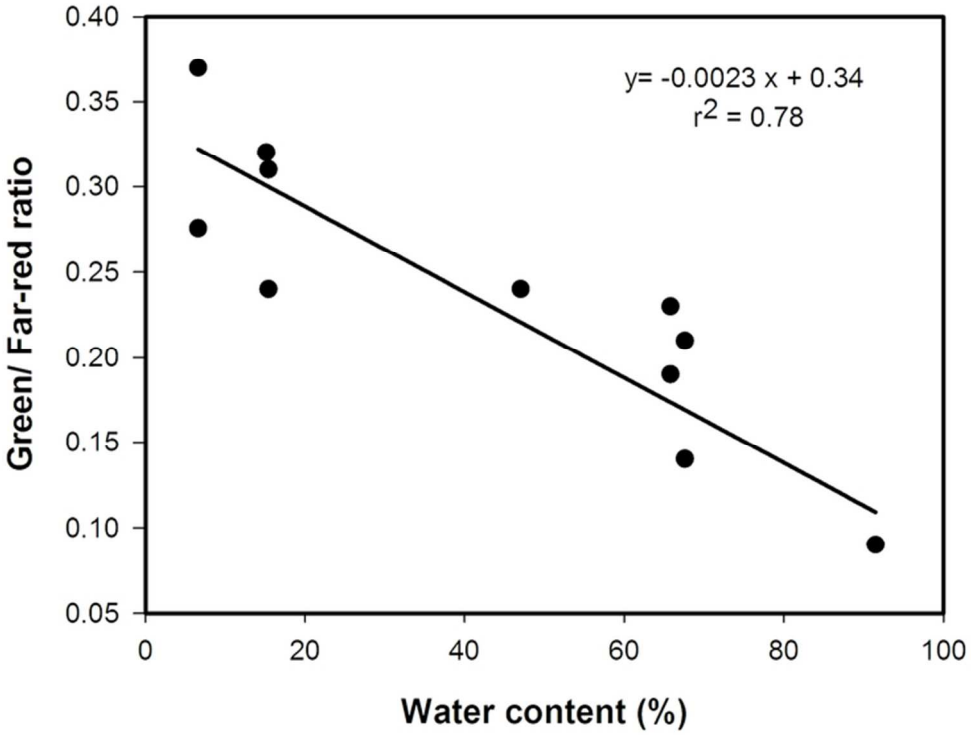

Figure 10. Green/ Far-red ratio as a function of water content (mass percentage) in oregano leaves.
64x49mm (300 x 300 DPI)

For Review

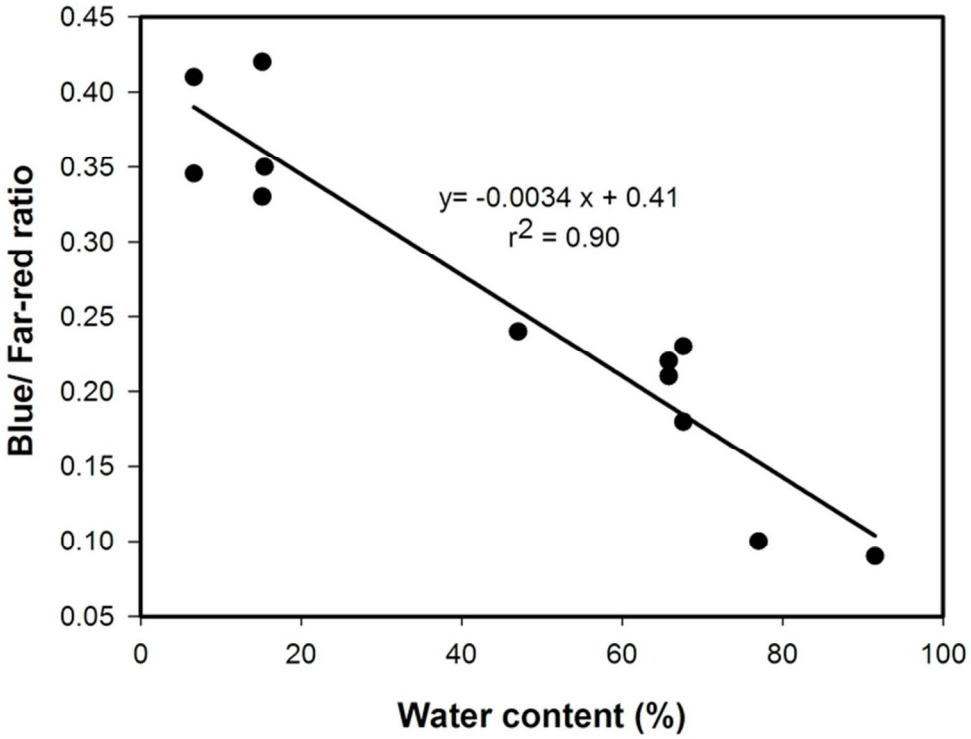

Figure 11. Blue/ Far-red ratio as a function of water content (mass percentage) in oregano leaves.
64x50mm (300 x 300 DPI)

For Review

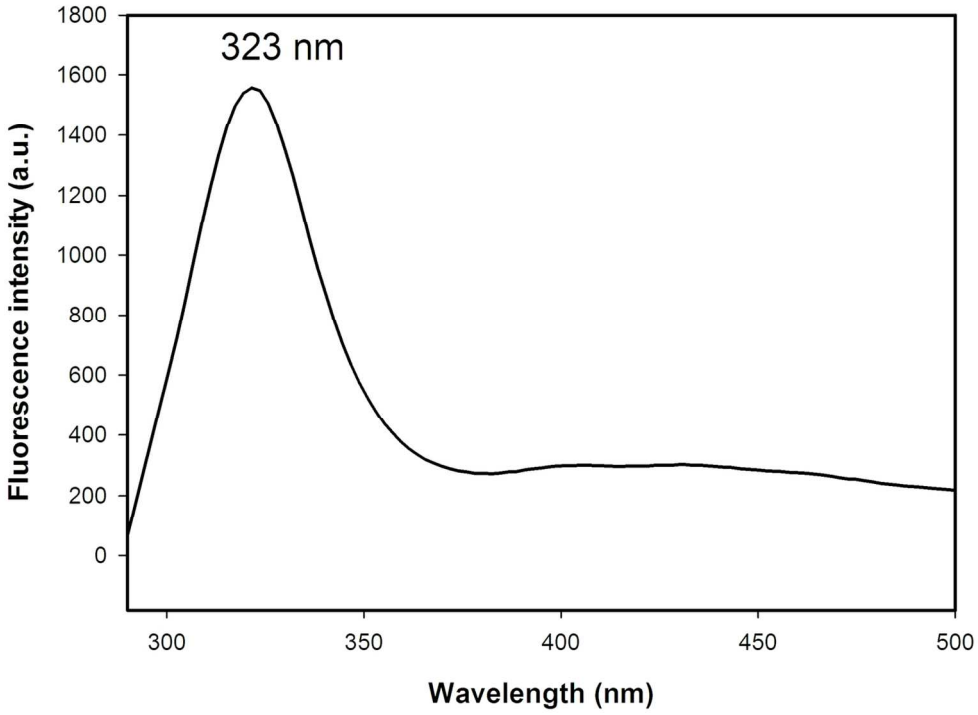

Figure 12. Fluorescence spectra corrected for the detector response for the essential oil of oregano in ethanol solution. Excitation wavelength: 275 nm
65x51mm (600 x 600 DPI)

Review

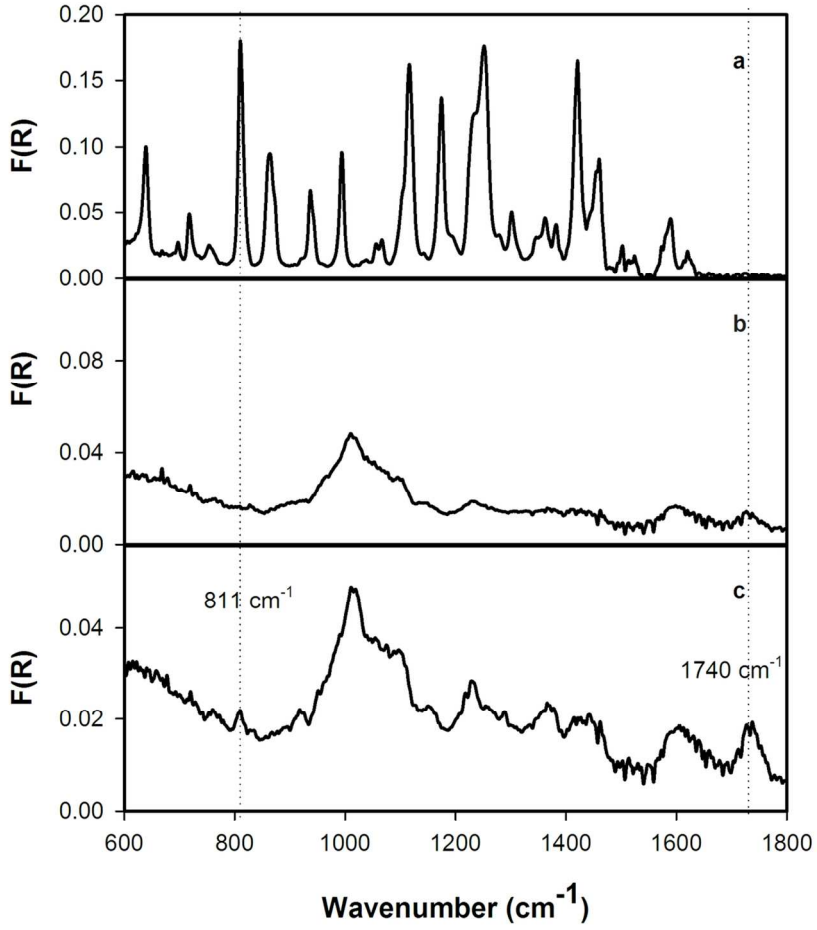

Figure 13. ATR-FTIR spectra for a) the essential oil of oregano distilled from leaves and inflorescences, b) dry leaves, c) dry inflorescences.
111x149mm (300 x 300 DPI)

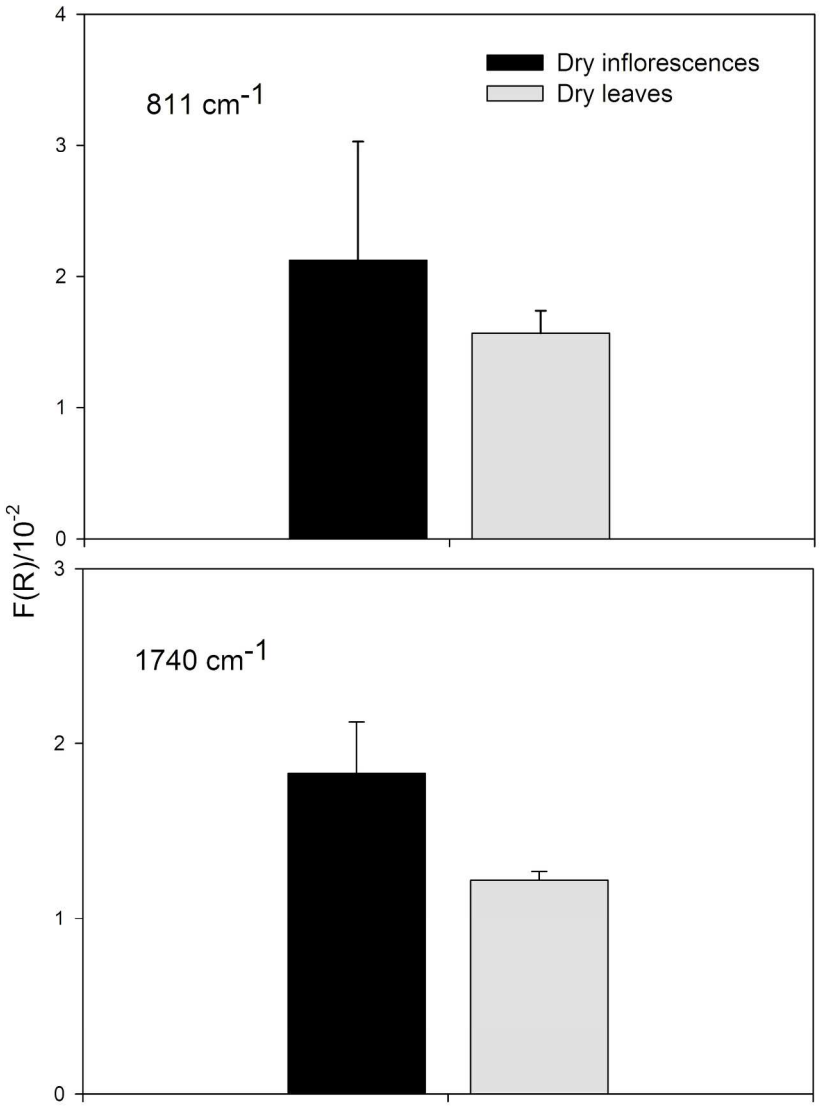

Figure 14. Absorption bands at 811 cm-1 and 1740 cm-1 from ATR-FTIR of dry inflorescences and dry leaves of oregano. The error bars represent the standard deviation
205x263mm (300 x 300 DPI)